applied sciences

MDPI

Article

Static Structures in Leaky Mode Waveguides †

Daniel Pettingill, Daniel Kurtz and Daniel Smalley *

Department of Electrical and Computer Engineering, Brigham Young University, Provo, UT 84602, USA; dptres16@gmail.com (D.P.); kurtz117@yahoo.com (D.K.)

* Correspondence: smalley@byu.edu; Tel.: +1-1-801-422-4343

† It is an invited paper for the special issue.

Received: 20 December 2018; Accepted: 7 January 2019; Published: 11 January 2019

Featured Application: The overarching contextual objective of this research is to create transparent, near-eye devices for holographic video display.

Abstract: In this work, we suggest a new method of expanding the field of view in bottom-exit, leaky mode devices for transparent, monolithic, holographic, near-eye display. In this approach, we propose the use of static, laser-induced, grating structures within the device substrate to break the leaky mode light into diffracted orders. We then propose to use carefully timed illumination pulses to select which diffracted order is visible to the eye at every display refresh interval (up to 100 kHz). Each of these orders becomes a view for a different image point. To describe this new method, we use K-vector analysis. We give the relevant equations and a list of parameters which lead to a near-eye geometry with little or no overlap in higher-order view zones. We conclude that it should be possible to increase the field of view of our bottom-exit, leaky mode devices by as much as one order of magnitude by simply adding a laser-induced grating structure to the substrate and by carefully timing the device illumination. If successful, this method would make possible a transparent, holographic, near-eye display that is simple to fabricate, relative to pixelated approaches, and which has a wide field-of-view relative to our current bottom-exit displays.

Keywords: near-eye display; leaky mode; lithium niobate; holographic video; augmented reality; 3D display; acousto-optic modulator; laser-induced structures

1. Introduction

This study is important to the use of leaky mode modulators as near-eye displays because it seeks to increase the device's field of view without making the fabrication of the device significantly more complex. Currently, near-eye displays are almost exclusively driven by pixelated spatial light modulators [1]. However, leaky mode modulators have a number advantages over pixelated spatial light modulators (SLMs) for the purposes of near-eye holographic display. They require only two mask steps to fabricate. They are transparent. They produce no zero order, no higher orders, and no conjugate images. They do not suffer from quantization error from pixilation, and they require no backplane. Additionally, they have the ability to rotate the polarization of the diffracted signal light for easy noise filtering. Finally, they can also multiplex color in the frequency domain, allowing all colors to be modulated in the same waveguide. However, these advantages notwithstanding, bottom-exit devices (the configuration most useful for near-eye display) suffer from a reduced field of view. In side-exit leaky mode devices, we observe a large multiplication of diffracted light angle because the device is operating in a regime where the grating equation is nonlinear [2,3]. In a bottom-exit device, leaky mode light passes through a high-spatial-frequency output grating that operates in opposition to the leaky mode diffraction [4]. This second interaction effectively erases the angle-multiplication

advantage gained from illuminating the acoustic holographic pattern at a glancing angle. The result of the reduction is that the leaky mode device effectively has a smaller achievable field of view (defined in this work as the visible extent at a given depth) or view zone (defined here as the angular extent over which a point is visible). Note that these concepts are duals in this context and will be treated interchangeably in the text. Our previous work identified the narrowing of view angle in bottom-exit devices as a challenge and stated that a solution would be described in a future publication [4]. The main aim of this work is to present that solution to restore or increase the leaky mode device view zone/field of view (see Figure 1) and/or view zone by temporally stitching together multiple diffracted orders of light created by a static internal grating.

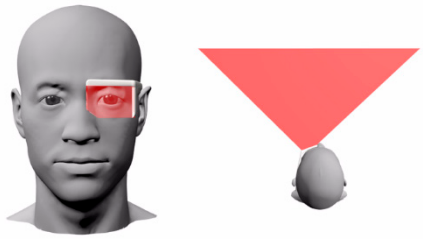

Figure 1. Low-profile near-eye display concept with a goal of large field of view.

Other researchers have used higher-order images to increase the display view zone, field of view, and space bandwidth product [5,6]. This work differs from previous efforts in several ways. First, our holographic pattern is a rapidly moving analog signal and not a pixel pattern with fixed locations. Also, leaky mode devices in near-eye applications can have an extremely high refresh rate—potentially exceeding 100 kHz for a 1 cm free-running surface acoustic wave (SAW) aperture (a leaky mode device can write a one millimeter aperture in approximately one microsecond). This refresh rate is at least two orders of magnitude higher than that of commercial near-eye displays and it allows us the ability to contemplate a line-rate approach to increasing field of view. Additionally, our leaky mode devices are made on a highly transparent lithium niobate substrate which is desirable for near-eye applications. Furthermore, using femtosecond laser pulses, we can create high-contrast, laser-induced gratings in the bulk of the substrate [7,8] with a number of diffracted orders of visible power. Finally, in addition to spatial light modulation, lithium niobate is an excellent electro-optic substrate which is frequently used to make fast (up to picosecond-rate) phase and amplitude modulators [9]. These unique attributes of a moving pattern, high refresh rate, high-contrast internal gratings, and integrated illumination pulsing are important to our proposed solution for increasing the field of view in bottom-exit leaky mode devices.

Leaky mode devices comprise a transparent slab of a piezoelectric substrate, such as lithium niobate, with a waveguide indiffused on the surface which sits adjacent to an interdigital transducer. When an RF signal excites the transducer, a surface acoustic wave is generated that travels across the surface of the waveguide. Light trapped in the waveguide, traveling contra-linearly or collinearly with the SAW pattern, may be mode-coupled from a guided mode to a leaky mode which can be steered and shaped by the SAW pattern to form a holographic image. The use of such a device in a near-eye application is shown in Figure 2. A chirped SAW pattern is generated by the transducer which is designed to mode couple light so that it appears to have originated from a point in space. The leaky mode light travels at a shallow angle through the substrate. This angle is usually very shallow, typically between 1° and 12° from parallel to the substrate surface. However, this angle can be modified by passing the leaky mode light from one substrate to another with another index (or the same index, but canted at an angle) thereby increasing the angle by an angular bias if desired (will assume an angular bias of 10° for the analysis in this paper). The lateral translation of the light ends at the bottom surface of the substrate where the light is out-coupled by a high-spatial frequency out-coupling grating usually patterned by interference lithography and etched into the substrate. This grating has only one diffracted order into the air (all others are evanescent) and toward the viewer's eye. The light

rays that reach the viewer's eye can be back cast to a distant image point. As the surface acoustic wave moves across the device's SAW aperture, the image point moves across the viewer's field of view. The illumination light in the waveguide pulses in coordination with this movement to draw or emit points as the image point 'cursor' travels. When it has completed its scan, a new SAW chirp pattern is generated with a different depth and the field of view that is scanned again for as many depth planes as desired (we recently demonstrated a device with arbitrary focus from 4 ft to 10 ft [4]). Several leaky mode waveguide/transducer 'channels' can be placed adjacent to one another to create a vertically multiplexed array. Each channel becomes responsible for the one line of the display. In this way, images can be created at multiple depth planes to form a 3D image.

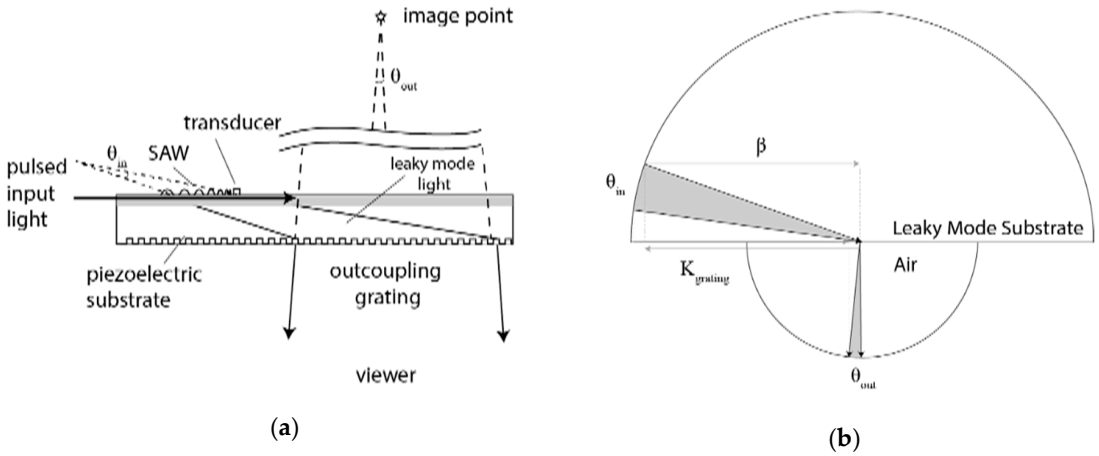

Figure 2. Reduction of view angel for bottom-exit leaky mode devices: (**a**) light diffracting from a surface acoustic wave (SAW) pattern is out-coupled with a grating; (**b**) The K-vector analysis shows a significant reduction in θ_{out} vs. θ_{in}. The former of these angles dictates the display view zone and field of view.

In this paper, we propose a simple modification to the leaky mode device by adding a laser-induced, static grating in the substrate of the leaky mode device. Femtosecond lasers can induce phase changes and 'catastrophic' lattice changes in the bulk of lithium niobate. The local nature of the change is aided by two photon up-conversion in the substrate. The result is that relatively high contrast gratings can be formed in the substrate with critical dimensions down below a micron and write depth of several tens of microns (see Figure 3). When coupled with high-accuracy, large-travel stages, whole wafers can be written with sub-surface gratings [10–12]. These gratings can be uniform, chirped, Raman–Nath, or Bragg grating. In our application, we explore a uniform thin grating underneath our leaky mode channels. It would be possible to have different periods underneath each channel, but for this analysis we will assume that the induced grating has only one period everywhere.

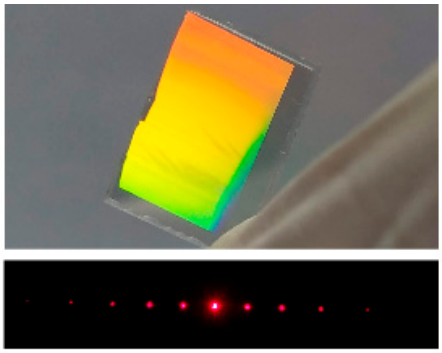

Figure 3. A laser-induced grating in x-cut lithium niobate and the resulting diffraction pattern with several high-order modes.

The purpose of the grating is to break the leaky mode light into different orders, each propagating at a different angle. These angles are determined by the laser-induced grating period. Depending on laser parameters, we have generated gratings with half a dozen or more orders. Our analysis assumes five such orders. Each of these diffracted orders will form a high-order image point that appears at a different location and is visible from a different angle than the original image point. We propose that these 'copies' of the original image point and others of different depths, can be superimposed over time to form a single image point, as illustrated in Figure 4a. Instead of scanning with just one point to form an image, now we scan with multiple points. We pulse only when one of these points is in a location that corresponds to a point location and a view in the target image (Figure 4b). Over time, as these spatial and angular ray bundles accumulate, a wide view angle for every point in the image is achieved (Figure 4c).

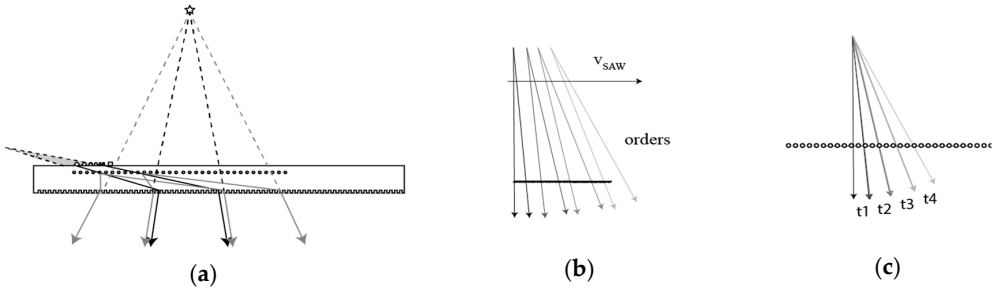

Figure 4. The multi-order leaky mode concept: (**a**) multiple orders combined to create a large view zone (or, alternatively, field of view). (**b**) Orders will travel across the display in front of the viewer. (**c**) The illumination is pulsed as orders pass by the viewer so multiple views are stitched into a wide view zone.

The success of this approach depends upon several of the unique features of leaky mode devices: high refresh rate, smoothly varying chirp functions, fast moving surface acoustic waves and translating leaky mode light. However, these attributes are not sufficient to make the approach successful if the view zones for each diffracted order cannot be adequately separated at the viewer's eye. If, for example, the viewer saw two overlapped view zones, they would see two points simultaneously and the display designer could not 'write' one point without also writing the other. Figure 5a shows a multi-order, HPO, hologram rendered in grayscale resist and reproduced with 633 nm light. Here, multiple images are created, one for each order of diffraction and each with a corresponding view zone (Figure 5b). Notice the overlap between the second- and third-order view zones. If the images appeared at different depths (which they do in this case), the viewer would see two images in the overlap position instead of one. Therefore, for our proposed multi-order method we must be able to eliminate as much as possible the overlap between adjacent view zone orders and achieve what we will call a 'no-overlap condition'. Below, we will use vector analysis to identify parameters for a 'no overlap condition', for a near-eye geometry.

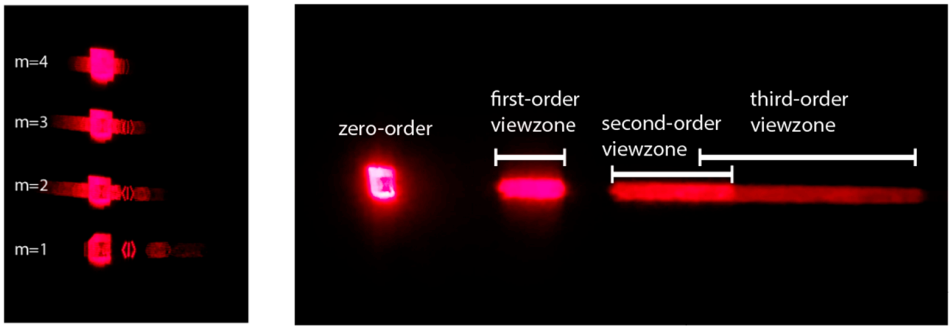

(**a**) (**b**)

Figure 5. High-order holographic images and view zones: (**a**) first through a fourth-order image for a horizontal parallax only (HPO) hologram. This hologram, created in grayscale photoresist, is meant to simulate the output of a leaky mode modulator passing through thin grating. (**b**) Here, we see how the high-order holographic view zones separate or overlap.

2. Supplies and Methods

The geometries for order overlap are shown in Figure 6a. We will use K-vector analysis to show the relationship between points P and Q. After choosing parameters for a near-eye geometry including an internal grating period, Λ_D, and propagation distance, d_3, we will plot the high-order rays to confirm a 'no-overlap' condition.

We start with the back-cast chirp focus point, $P = (x_0, z_0)$. This parameter is a function of the leaky mode drop angle, θ, whose value will change along the chirp. We can use the angles, θ_0 and θ_1 of light rays exiting both ends of the SAW chirp to define two vectors:

$$\overline{k_0} = k_{sub}\sin(\theta_0)\hat{x} + k_{sub}\cos(\theta_0)\hat{z} \text{ and} \tag{1}$$

$$\overline{k_1} = k_{sub}\sin(\theta_1)\hat{x} + k_{sub}\cos(\theta_1)\hat{z}, \tag{2}$$

$$\text{where } k_{sub} = \frac{2\pi n_{ord}}{\lambda_0}. \tag{3}$$

We take the substrate index of refraction as $n_{ord} = 2.2864$ for $\lambda_0 = 633$ nm [13]. Conservation of transverse momentum preserves the value of the vector components parallel to the device interfaces. Therefore, in our analysis we keep track of the propagation constants:

$$\beta_0 = k_{sub}\sin\theta_0 \tag{4}$$

$$\beta_1 = k_{sub}\sin\theta_1 \tag{5}$$

The analysis can be thought of as having multiple layers separated in depth. They are as follows: d_1, the absolute distance from the chirp focus point to the SAW plane; d_2, the absolute distance from the SAW plane to the laser-induced internal grating; d_3, the absolute distance from the internal grating to the output grating; and d_4, the absolute distance traveled by light through the air to the viewer's eye (see Figure 6a).

The vectors $\overline{k_0}$ and $\overline{k_1}$ bracket a ray bundle that propagates through each device layer toward the eye. The cross section of the ray bundle at each of these layers is:

$$\Delta x^{i} = x_1^{i} - x_0^{i} \text{ where } x_1^{i} = d_1\tan\theta_1, \text{ and } x_0^{i} = d_1\tan\theta_0 \tag{6}$$

$$\Delta x^{ii} = x_1^{ii} - x_0^{ii},\ x_1^{ii} = (d_1+d_2)\tan\theta_1, \text{ and } x_0^{ii} = (d_1+d_2)\tan\theta_0 \tag{7}$$

$$\Delta x^{iii} = x_1^{iii} - x_0^{iii},\ x_1^{iii} = (d_1+d_2+d_3)\tan\theta_1, \text{ and } x_0^{iii} = (d_1+d_2+d_3)\tan\theta_0 \tag{8}$$

$$\Delta x^{iv} = x_1^{iv} - x_0^{iv},\ x_1^{iv} = (d_1+d_2+d_3+d_4)\tan\theta_1, \text{ and } x_0^{iv} = (d_1+d_2+d_3+d_4)\tan\theta_0 \tag{9}$$

In order to calculate the final orientation of $\overline{k_0}$ and $\overline{k_1}$ after they have passed through both the internal grating and the output coupling grating for every order N, we simply subtract K_G once (every exiting ray must be diffracted by the output grating) and subtract (for negative orders) K_D, N times (see Figure 6b). The magnitudes of the parallel components for the resulting k-vectors are,

$$k_{0,||} = \beta_0 + mNK_D - K_G, \text{ and} \tag{10}$$

$$k_{1,||} = \beta_1 + mNK_D - K_G, \tag{11}$$

where m determines the sign of the diffracted orders; $m = -1$ in this paper. Using coordinate geometry, we determine that u_N and v_N can be expressed as:

$$u_N = \frac{x^{iii}_{0,N} M_{0,N} - x^{iii}_{1,N} M_{1,N}}{M_{0,N} - M_{1,N}} \text{ and} \tag{12}$$

$$v_N = (u_0 - x^{iii}_{1,N}) M_{1,N} - (d_1 + d_2 + d_3) \text{ where,} \tag{13}$$

$$M_{0,N} = \frac{k_{0,N,\perp}}{k_{0,N,||}} = \frac{\sqrt{k^2_{air} - (\beta_0 + mNK_D - K_G)^2}}{(\beta_0 + mNK_D - K_G)} \text{ and} \tag{14}$$

$$M_{1,N} = \frac{k_{1,N,\perp}}{k_{1,N,||}} = \frac{\sqrt{k^2_{air} - (\beta_1 + mNK_D - K_G)^2}}{(\beta_1 + mNK_D - K_G)} \tag{15}$$

We define the non-overlap condition for order when the view zones are $x^{iv}_{1,1} < x^{iv}_0$ (i.e., the first $m = -1$ diffraction of $\overline{k_1}$ is below the $m = 0$ order of $\overline{k_0}$ at the viewing distance). For the non-overlap condition to be satisfied at any distance, K_D must be greater than $\Delta\beta = \beta_1 - \beta_0$.

To determine the distance, d_4, at which the non-overlap condition is satisfied, we must find the intersection of two lines. We compose the first ray from the slope of the un-diffracted $\overline{k_0}$ vector and the coordinates of the point, $[x^{iii}_0, -(d_1, d_2, d_3)]$. We compose the second ray from the slope of the negative first-order diffracted, $\overline{k_1}$ vector and the coordinates of the point, $[x^{iii}_{1,1}, -(d_1, d_2, d_3)]$. We solve for the intersection of these two lines to obtain,

$$z_{int} = (x_{int} - x^{ii}_1) M_{1,int} - (d_1 + d_2) \text{ where,} \tag{16}$$

$$x_{int} = \frac{x^{iii}_0 M_{0,int} - x^{iii}_1 M_{1,int}}{M_{0,int} - M_{1,int}}, \tag{17}$$

$$M_{0,int} = \frac{k_{0,\perp}}{k_{0,||}} = \frac{-\sqrt{k^2_{sub} - \beta^2_0}}{\beta_0}, \tag{18}$$

$$M_{1,int} = \frac{k_{1,-1,\perp}}{k_{1,-1,||}} = \frac{-\sqrt{k^2_{sub} - (\beta_1 - K_D)^2}}{(\beta_1 - K_D)}. \tag{19}$$

Note that the slopes in this case have perpendicular k components traveling in the opposite direction of those in Equations (14) and (15) above. This is because these rays are going down rather than up.

The coordinate, z_{int}, gives the depth *within* the material at which the zero and first-order views separate. This is a higher than necessary upper bound as the two orders still have additional time to separate as they propagate through distance, d_4. However, this provides time for other orders, that may have stronger overlap, to separate and to form a set of view windows that is well-separated at the viewing plane.

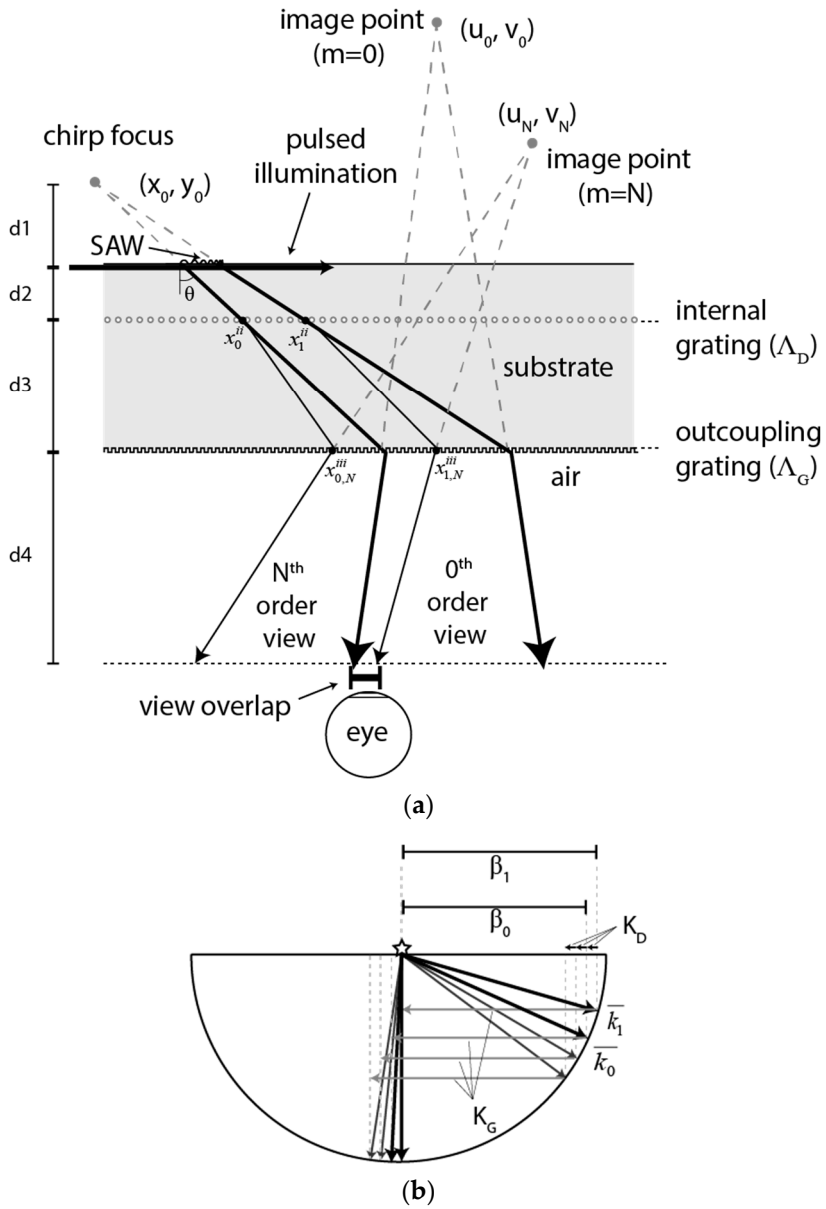

Figure 6. Multiple-order leaky mode concept: (**a**) leaky mode light diffracts into multiple orders within the substrate to form multiple image points at different angles and visible from different angles. (**b**) The K-vector analysis showing momentum change for both the internal grating and the out-coupling grating.

We chose the parameters listed in Table 1 to define our near-eye geometry. We chose a 6 mm (d_2 = 1 mm + d_3 = 5 mm) thick substrate with an internal grating at a 1mm distance from the SAW layer with a period, Λ_D, of approximately 4 μm and an output coupling grating with a period, Λ_G of approximately 300 nm. These values correspond to $K_D \approx 2 * \Delta\beta$ and $K_G \approx \beta_0$, respectively. An approximately 10° bias was assumed to give maximum and minimum leaky mode angles of $\theta_0 = 70°$ and $\theta_1 = 77°$. All of these fit within reasonable fabrication parameters for a two-substrate system.

Table 1. Near-eye parameters.

Parameter	Value	Notes
λ_{air}	633 nm	–
θ_0	70°	10° bias
θ_1	77°	10° bias
K_D	1.58×10^6	$2\Delta\beta$
K_G	2.1×10^7	$\approx \beta_0$
Λ_D	3.99 µm	Internal grating
Λ_G	295 nm	Output grating
N	5	modes (neg.)
n_{ord}	2.2864	$LiNbO_3$
d_1	1 mm	chirp focus
d_2	1 mm	to grating 1
d_3	5 mm	to grating 2
d_4	20 mm	to viewer

3. Results

The results of our analysis, run in Matlab for five negative orders, are shown in Figure 7 and Table 2. The no-overlap condition was met such that there was little or no overlap of view-zones (Figure 7a). The minimum no-overlap window was calculated to be 5.9 mm and the pulse timings to align these windows are given in Table 2. Figure 7b shows that the higher-order diffraction added 52.5° of view zone/field of view to the zero-order view zone/field of view of 4.5° to make a total of 57°—a more than ten-fold increase in the near-eye case. For $K_D \approx 2\Delta\beta$, the angular duty cycle is 50% for one light traveling in only one direction (see discussion).

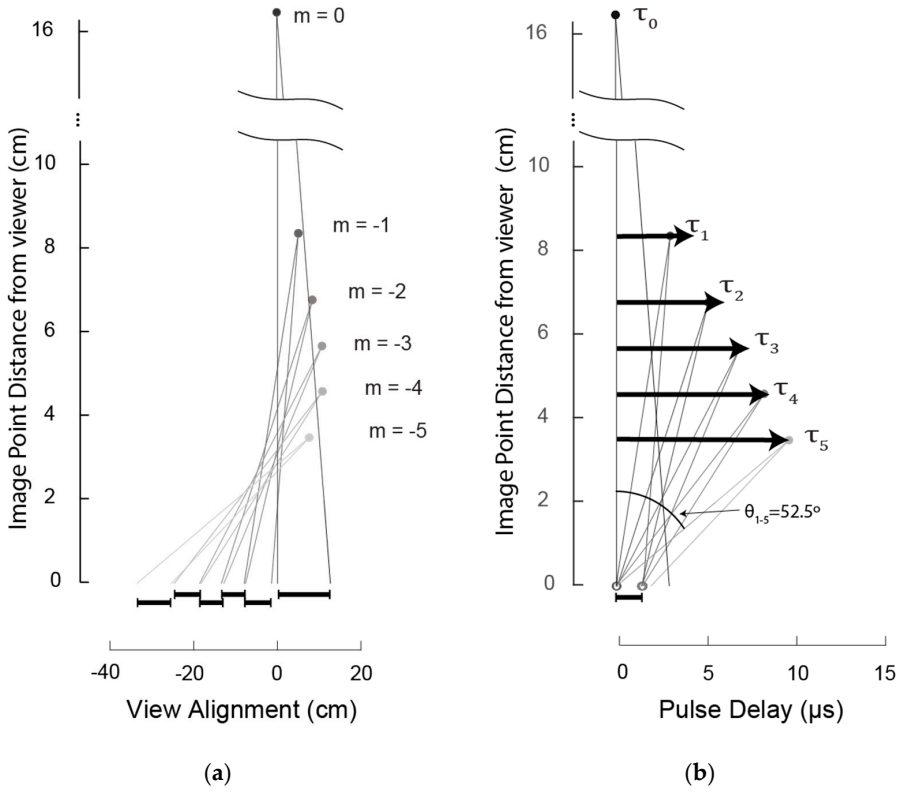

(**a**) (**b**)

Figure 7. Results of view angle and pulse delay calculations for the parameters in Table 1: (**a**) The five negative orders used show little or no overlap at the viewer. (**b**) The non-zero view angles aggregate to a total of 52.5°. The relative pulse delay times are shown to all be under 10 µs.

Table 2. View window and pulse delay for image points corresponding to diffracted orders.

Order	View Window (mm)	Pulse Delay (μs)
0	13.0	0
−1	6.6	2.1
−2	5.9 [1]	3.6
−3	5.9 [1]	5.1
−4	6.7	6.8
−5	9.2	9.6

[1] These smallest windows define the total view window for the eye.

4. Discussion

The above results show that the multi-order leaky mode devices have the potential to create image points with a ten-fold increase in the view zone and/or field of view. They show that the non-overlap condition can be achieved for the near-eye case with parameters that are within the current fabrication limits for leaky mode devices, femtosecond direct-writing and interference lithography. The minimum view window of 5.9 mm is larger than the average pupil diameter of the eye and can be actively positioned in front of the pupil, if desired. All pulse delay times are under 10 μs and correspond to roughly 10 mm of SAW travel on the device surface. This means that a new pattern can be written at a rate of approximately 100 kHz. Therefore, to address all of these orders, the SAW would have to travel the SAW chirp length (typically between 1 mm and 10 mm) plus 10 mm. This distance is well-matched to the SAW aperture of current leaky mode devices.

The dramatic increase of view zone from 4.5° to 57° has some important context. Because we chose $K_D \approx 2\Delta\beta$ instead of $K_D \approx \Delta\beta$, the resulting ray bundles are not continuous in angle. Instead, the angular views have gaps that result in a 50% angular duty cycle. We could theoretically choose a very high K_D and achieve a nominal view angle approaching 90 or even 180 degrees, but as long as we only use five modes, the active portions of that view angle would only come to a total of between 25° and 30°, regardless of the total view angle. However, there are ways of filling these gaps, aside from using more modes. We could, for example, run a second channel with light traveling in the opposite direction. The result would be the *interlacing* of the output views to create a continuous sweep of views. In this scenario, the additional channel could use the same waveguide, the same grating structures, even the same *transducer*, if desired, (because ITDs are inherently bi-directional). In this scenario, the internal grating could remain the same and the output grating period would be increased (and made simpler to fabricate) so that the fan of angles was symmetric around the surface normal. The result would be a smooth set of views across the 57° sweep without greatly increasing fabrication complexity.

It is worth restating a few of these points. In our methodology, we chose K_G to select which order will be directed normal to the output face. For example, by setting $K_G = \beta_1 - 3K_D$ (the third-order diffraction of the $\overline{k_1}$), we obtain an aggregate sweep that is roughly symmetric and ready for the interlacing described above. If, instead, we choose $K_G = \beta_1$, we obtain a unilateral spread that would be ideal for combining with another unilateral spread. This would be the ideal configuration if the sweep were continuous in angle. However, continuity would require that $K_D \approx \Delta\beta$, which would make it impossible to eliminate view zone overlap. It should be noted, however, that this overlap would be less important for viewers far away from the device (e.g., 500 mm). Therefore, looking forward, this approach might also be of special interest not only to near-eye displays but to large flatscreen displays as well.

5. Conclusions

We have described a new approach to increasing the view zone in leaky mode devices. We have shown the results of an analysis that suggests the existence of at least one set of parameters for a multi-order, near-eye, leaky mode device with viewzones that have little or no overlap. It may now

be possible to increase the effective view zone or field of view for of a multi-order leaky mode device more than ten-fold.

Author Contributions: Conceptualization, D.S.; Software, D.P., D.K., D.S.; methodology, D.P., D.S.

Funding: This research was funded by Air Force Research Laboratory contract FA8650-14-C-6571.

Conflicts of Interest: The authors declare no conflict of interest.

References

1. Smalley, D.E.; Smithwick, Q.Y.J.; Bove, V.M.; Barabas, J.; Jolly, S. Anisotropic leaky-mode modulator for holographic video displays. *Nature* **2013**, *498*, 313–317. [CrossRef] [PubMed]
2. Qaderi, K.; Leach, C.; Smalley, D.E. Paired leaky mode spatial light modulators with a 28° total deflection angle. *Opt. Lett.* **2017**, *42*, 1345–1348. [CrossRef] [PubMed]
3. Qaderi, K.; Smalley, D.E. Leaky-mode waveguide modulators with high deflection angle for use in holographic video displays. *Opt. Express* **2016**, *24*, 20831–20841. [CrossRef] [PubMed]
4. McLaughlin, S.; Henrie, A.; Gneiting, S.; Smalley, D.E. Backside emission leaky-mode modulators. *Opt. Express* **2017**, *25*, 20622–20627. [CrossRef] [PubMed]
5. Lee, B.; Li, G.; Hong, J.-Y.; Lee, D.; Yeom, J. Viewing zone enlargement of holographic display using high order terms guided by holographic optical element. In *Propagation through and Characterization of Distributed Volume Turbulence and Atmospheric Phenomena*; Optical Society of America: Washington, DC, USA, 2015; Volume 24, p. JT5A.
6. Li, G.; Jeong, J.; Lee, D.; Yeom, J.; Jang, C.; Lee, S.; Lee, B. Space bandwidth product enhancement of holographic display using high-order diffraction guided by holographic optical element. *Opt. Express* **2015**, *23*, 33170–33183. [CrossRef] [PubMed]
7. Burghoff, J.; Grebing, C.; Nolte, S.; Tünnermann, A. Efficient frequency doubling in femtosecond laser-written waveguides in lithium niobate. *Appl. Phys. Lett.* **2006**, *89*, 081108. [CrossRef]
8. Thomson, R.; Campbell, S.; Blewett, I.; Kar, A.; Reid, D. Optical waveguide fabrication in z-cut lithium niobate ($LiNbO_3$) using femtosecond pulses in the low repetition rate regime. *Appl. Phys. Lett.* **2006**, *88*, 111109. [CrossRef]
9. Wang, C.; Zhang, M.; Chen, X.; Bertrand, M.; Shams-Ansari, A.; Chandrasekhar, S.; Winzer, P.; Loncar, M. Integrated lithium niobate electro-optic modulators operating at CMOS-compatible voltages. *Nature* **2018**, *562*, 101. [CrossRef] [PubMed]
10. Gattass, R.R.; Mazur, E. Femtosecond laser micromachining in transparent materials. *Nat. Photonics* **2008**, *2*, 219. [CrossRef]
11. Savidis, N.; Jolly, S.; Datta, B.; Karydis, T.; Bove, V.M. Fabrication of waveguide spatial light modulators via femtosecond laser micromachining. In *Advanced Fabrication Technologies for Micro/Nano Optics and Photonics IX*; International Society for Optics and Photonics: San Diego, CA, USA, 2016; Volume 9759, p. 97590R.
12. Burghoff, J.; Nolte, S.; Tünnermann, A.J.A.P.A. Origins of waveguiding in femtosecond laser-structured $LiNbO_3$. *Appl. Phys. A* **2007**, *89*, 127–132. [CrossRef]
13. Zelmon, D.E.; Small, D.L.; Jundt, D. Infrared corrected Sellmeier coefficients for congruently grown lithium niobate and 5 mol.% magnesium oxide–doped lithium niobate. *JOSA B* **1997**, *14*, 3319–3322. [CrossRef]